*Cell Transplantation*, Vol. 21, pp. 2735–2751, 2012


0963-6897/12 $90.00 + .00
DOI: http://dx.doi.org/10.3727/096368912X637497
E-ISSN 1555-3892
www.cognizantcommunication.com

# Genipin-Cross-Linked Microencapsulated Human Adipose Stem Cells Augment Transplant Retention Resulting in Attenuation of Chronically Infarcted Rat Heart Fibrosis and Cardiac Dysfunction

Arghya Paul,* Guangyong Chen,† Afshan Khan,* Vijayaraghava T. S. Rao,‡ Dominique Shum-Tim,† and Satya Prakash*

*Biomedical Technology and Cell Therapy Research Laboratory, Department of Biomedical Engineering and Artificial Cells and Organs Research Centre Faculty of Medicine, McGill University, Montreal, Québec, Canada
†Divisions of Cardiac Surgery and Surgical Research, McGill University Health Center, Montreal, Quebec, Canada
‡Institute of Parasitology, McGill University, Macdonald Campus, Ste. Anne de Bellevue, Quebec, Canada

Stem cell transplantation has been widely acknowledged for their immense potential in regenerative medicine. In these procedures, the implanted cells need to maintain both their viability and functional properties for effective therapeutic outcomes. This has long been a subject of major concern and intensive studies. Microencapsulation of stem cells within polymeric microcapsules can be an efficient approach to achieve this goal, particularly for heart diseases. This study reports the use of biocompatible, fluorogenic genipin-cross-linked alginate chitosan (GCAC) microcapsules in delivery of human adipose stem cells (hASCs) with an aim to increase the implant retention in the infarcted myocardium for maximum clinical benefits. In vitro results show, under hypoxic conditions, the microencapsulated cells overexpressed significantly higher amount of biologically active vascular endothelial growth factor (VEGF). We investigated on the in vivo potential using immunocompetent female rats after induction of myocardial infarction. For this, animal groups ($n=8$) received empty control microcapsules, $1.5\times10^6$ free male hASCs, or $1.5\times10^6$ microencapsulated male hASCs. Results show significant retention (3.5 times higher) of microencapsulated hASCs compared to free hASCs after 10 weeks of transplantation. Microencapsulated hASCs showed significantly attenuated infarct size compared to free hASCs and empty microcapsule group (21.6% ± 1.1% vs. 27.2% ± 3.1% vs. 33.3% ± 3.2%; $p<0.05$), enhanced vasculogenesis, and improved cardiac function (fractional shortening: 24.2% ± 2.1% vs. 19.1% ± 0.5% vs. 12.0% ± 4.0%; $p<0.05$). These data suggest that microencapsulated hASCs can contribute significantly to the improvement in cardiac functions. Their greater retentions exhibit reduced fibrosis and cardiac dysfunction in experimental animals. However, further research is needed to fully comprehend the underlying biological and immunological effects of microencapsulated hASCs, which jointly play important roles in cardiac repair.

Key words: Cell transplant; Adipose stem cell therapy; Tissue engineering; Myocardial infarction; Microencapsulation; Regenerative medicine

## INTRODUCTION

Cardiovascular diseases, such as cardiomyopathy and ischemic heart diseases, are a major cause of concern all over the world (11). Ischemic heart disease refers to the decrease in oxygenated blood flow to the myocardium or heart muscle, which leads to an inadequate supply of oxygen to the cardiac muscle eventually leading to a permanent damage to the cardiomyocytes followed by myocardial infarction (20). Stem cell transplantation has been considered as a major breakthrough in treating such diseases. Although the majority of cardiovascular research in stem cell therapy has involved bone marrow-derived mesenchymal stem cells (BMSCs), human adipose stem cells (hASCs) are an ideal alternative and as a result have been researched extensively as of late (35,36,45). Adipose tissue, like bone marrow, is derived from the mesenchyme. Therefore, ASCs also have the potential to differentiate into mesodermal lineages. ASCs provide the same multipotency as BMSCs and even yield a higher cell number from the same amount of starting

Received November 25, 2010; final acceptance November 10, 2011. Online prepub date: April 10, 2012.
Address correspondence to Satya Prakash, Biomedical Technology and Cell Therapy Research Laboratory, Department of Biomedical Engineering and Artificial Cells and Organs Research Centre Faculty of Medicine, McGill University, 3775 University Street, Montreal, Québec, H3A 2B4, Canada. Tel: +1-514-398-3676; Fax: +1-514-398-7461; E-mail: satya.prakash@mcgill.ca

material (37). The safe expendability of this tissue allows for large quantities of stem cells to be harvested without difficulty and at minimal risk (9). Owing to their potency and relative abundance, ASCs may be the most promising and ideal stem cell studied to date (10,21,27). Moreover, ASCs also have natural ability to secrete vascular endothelial growth factors and induce angiogenesis, where the newly formed vessels help in recovery of the blood flow in the damaged tissues, eventually leading to increased oxygen availability (36).

Survival of cells after intramyocardial injection is crucial to the efficacy of therapeutic cell transplantation. Recent studies suggest that a massive mechanical loss of cells takes place in the first minutes after direct intramyocardial injection (23,33,40). Similar problems were also noticed by another group where both ASCs and MSCs could not survive in the harsh cardiac environment, resulting in acute transplanted cell death and subsequent loss of cardiac function (41). In light of the early time frame in which this cell loss takes place, it is unlikely that it happens only because of instant cell death of the transplanted cells. As the heart differs from other organs in that it is constantly contracting, it is possible that this may contribute to the mechanical loss by squeezing the injected cells out of the myocardium. As a result, the cells retained in the myocardium immediately after injection represent only a fraction of those initially implanted. It is from this subset that biological loss can then affect the remaining number of surviving cells.

Extensive research has been dedicated towards the development of efficient cell delivery systems that could promote tissue regeneration. Several cell immobilization techniques have been studied such as 3D scaffolds and gel-based entrapment carriers, but none has actually gained acceptance into the market (1,24,47,49). With these drawbacks and requirements in mind, studies led to the development of better techniques of cell delivery involving cell encapsulation within semipermeable microcapsules (7,8,15,30,51). This technique provides the advantage of localized cell retention, which in turn facilitates the release of therapeutic agents for prolonged time periods at the target site, increasing potential impact in tissue regeneration applications. As shown in our previous studies, the use of polymeric microcapsules can provide an efficient delivery system for the transplantation of mesenchymal stem cells and help in cell-based gene therapy for overexpression of the therapeutic proteins (29).

Current study focuses on increasing the retention of the transplanted cells at target site with minimum mechanical and biological loss. Reducing the myocardial loss of cells will increase the retention of higher number of viable cells at the target site, which can eventually reduce the cardiac dysfunction. Here, we hypothesized that cell delivery using biodegradable polymeric microcapsules will be a potential tool to achieve this goal (Fig. 1). This is because when the size of the injectate is larger than the blood vessel diameter, like that of microcapsules, the contractive forces of the heart will be unable to wash out the latter into the blood stream. On the contrary, with free cell delivery system, the pressure generated by the injection coupled with that generated by the beating heart easily forces the grafted cells through the disrupted blood vessels into the systemic circulation. Moreover, the capsular membrane will also protect the cells against the external harsh microenvironment and foreign bodies in the myocardium.

We have recently demonstrated, using fluorescent microspheres (diameter: 10 μm, impersonating the cells) encapsulated in standard 200 μm alginate poly-L-lysine microcapsules, that microcapsules can reduce the initial mechanical loss of microspheres in the beating heart as detected after 20 min of myocardial transplantation in the left ventricle of infarcted rat heart model (2,28). We have also reported the use of genipin, a highly biocompatible and naturally derived iridoid glucoside from Gardenia fruits, for covalent cross-linking outermost coating of the microcapsule membrane for live cell encapsulation and characterized the microcapsule structure and key physical characteristics including mechanical properties, resistance, permeability, and durability (7,8). In this article for the first time, we explore the potential of these new genipin-cross-linked alginate chitosan (GCAC) microcapsules in vivo for myocardial xenotransplantation in infarcted rat heart using hASCs and assess their ability to improve the cardiac function and diminish scar formation.

## MATERIALS AND METHODS

### *Chemicals*

Low-viscosity alginic acid sodium salt from brown algae (viscosity: ~250 cP, 2% in water at 25°C) and poly-L-lysine hydrobromide (PLL; molecular weight: 27,400) were bought from Sigma Chemicals (St. Louis, MO). Chitosan (low viscosity, $Mv = 7.2 \times 10^4$ by viscometry, degree of deacetylation at 73.5% by titration) and genipin were purchased from Wako BioProducts, USA.

### *Cell Culture*

Human ASCs ($n = 1$ male donor) were obtained from Invitrogen and cultured in Dulbecco's modified Eagle's medium (DMEM; Invitrogen) supplemented with 10% fetal bovine albumin (FBS). The cells were routinely maintained as stationary cultures in 75-$cm^2$ tissue culture flasks and incubated at 37°C in a controlled environment with an air atmosphere of 5% $CO_2$. Human umbilical vein endothelial cells (HUVECs)

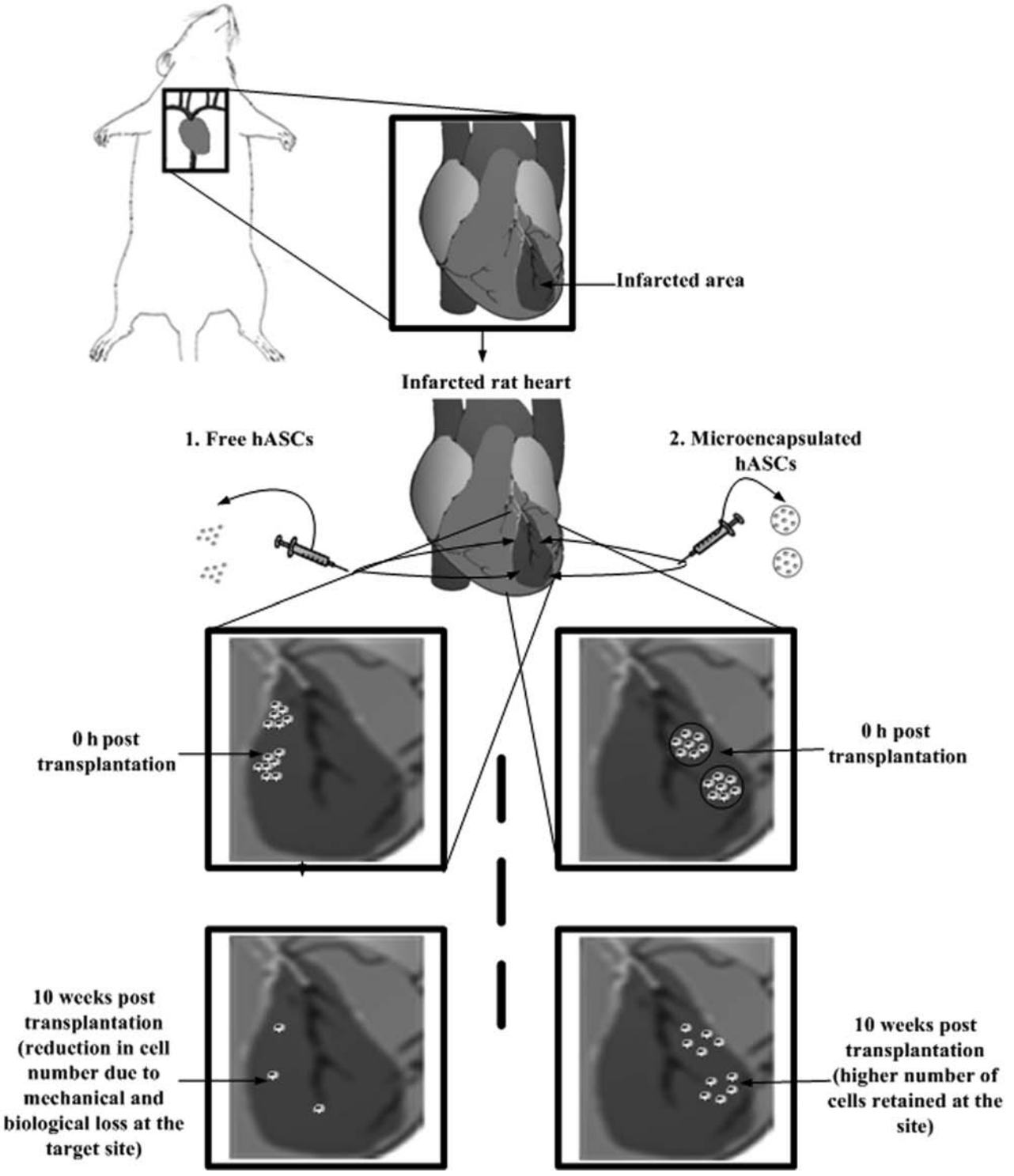


**Figure 1.** Schematic representation of direct intramyocardial delivery of microencapsulated adipose stem cells (hASCs) at the peri-infarct sites in comparison to free hASCs. We hypothesized that compared to nonencapsulated free hASCs (Method 1), the microencapsulated hASCs (Method 2) can better retain the transplanted cells at the infarct site, reduce massive mechanical cell washouts into microcirculation, and inhibit biological cell losses induced by the beating heart. The higher retention of transplanted viable cells at the infarct site (in this study, 10 weeks post transplantation) can eventually facilitate superior functional improvement of the infarcted heart.

(Sciencell, Carlsbad, CA, USA) were cultured and expanded on tissue culture flasks according to the supplier's instructions. They were cultured in endothelial cell medium (ECM) (Sciencell) supplemented with 5% FBS and placed in an incubator containing 5% $CO_2$ at 37°C.

*Preparation of GCAC Microcapsules Containing hASCs*

Calcium-alginate beads containing ASCs were generated using an encapsulator (Inotech Corp) with a 300-μm nozzle, which dispenses droplets of 1.5% sodium alginate solution containing cells ($1\times10^6$ cells/ml) into a constantly stirring solution of 0.1 M $CaCl_2$. After 20 min of stirring, the newly generated beads were coated with a chitosan layer by immersing them in a chitosan solution (2%) for 30 min. Subsequently, the beads were washed twice in 0.9% saline solution and immersed in genipin solution (5 mg/ml) for 12 h at 37°C to promote cross-linking with the chitosan layer. This was followed by rapid chelation of the inner alginate core of the microcapsules by incubating them in 0.055 mol/L sodium citrate solution for 5 min, followed by two washes in saline solution. To confirm the genipin cross-linking to the chitosan layer, the microcapsules were placed in a chambered coverglass system (Lab-Tek) under Laser Scanning Confocal Imaging System (LSM 510, Carl Zeiss, Jena, Germany) equipped with a Zeiss Axiovert 100M microscope. A 488-nm argon laser was used in the single green fluorescence mode, and the fluorescence was detected with the emission filter block BP500-550IR. Genipin reacts with amino terminals of the chitosan layer to emit green fluorescence on the outer surface of the capsule (8). After reaction confirmation, resulting microcapsules were thoroughly washed, replenished with fresh media to promote cell growth, and placed in a 37°C incubator containing 5% $CO_2$.

*Scanning Electron Microscope: Internal Morphology of the hASC Containing Microcapsule*

The internal morphology of the microencapsulated cells was studied by scanning electron microscopy (SEM) using a Hitachi S-4700 FE scanning microscope. The samples for SEM were prepared by rinsing the capsules with water, followed by freeze-drying and fracturing by a razor blade. The obtained fragmented halves of the microcapsules were mounted on a SEM stud with double-sided tape and sputter-coated with gold–palladium for 40 s.

*Detection of Viable Encapsulated Cells Using Stably Transduced LacZ Containing hASCs*

In order to assess the viability of the encapsulated cells hASCs were transduced with retroviral vector containing the LacZ gene before encapsulation. X-gal staining was used from time to time to indicate the viability of the LacZ-infected cells inside the GCAC microcapsules for 1 month.

*Assessment of Viability of Encapsulated Cells Using Dual Cell Staining*

Viability of the ASCs within the GCAC microcapsules was assessed using the polyanionic acetomethoxy derivate of calcein (calcein AM) and ethidium homopolymer EthD-III dyes (Biotium, Inc., Hayward, CA, USA) (29). The live cells were detected by the intracellular esterase mediated conversion of nonfluorescent cell-permeant calcein AM to fluorescent green calcein. The dead cells were detected by the bright red fluorescence emitted by EthD-III dye, which enters dead cells only through their damaged membranes and binds to nucleic acids. For this, the microcapsules were washed twice with PBS for 10 min each and resuspended in fresh PBS. Calcein AM (2 μM) and EthD-III (4 μM) were then added to the microcapsules and the microcapsules were incubated for 1 h before being examined under the fluorescent microscope.

*Induction of Hypoxic and Normoxic Conditions and Quantification of Released VEGF From Encapsulated hASCs*

hASCs were encapsulated in microcapsules, as described above, and grown for 24 h so as to allow them to stabilize in the new environment. Similarly, equal number of free cells was cultured in a stationary flask. On the following day, the media from the cultures were replaced with fresh media containing 10% FBS and the flasks were placed in either normoxic (21% $O_2$) or hypoxic (1% $O_2$) conditions for 24, 48, or 96 h. To induce hypoxic condition, a modular incubator chamber from Billup-Rothenberg, Inc., was used as mentioned elsewhere (32). At the end of the incubation period, the conditioned media from culture flasks were collected. Conditioned media from the culture flasks were collected, and the vascular endothelial growth factor (VEGF) release was quantified using a VEGF ELISA kit (R&D Systems) according to manufacturer's protocol. The data were represented as mean ± standard deviation (SD).

*Evaluation of Bioactivity of Conditioned Media of Encapsulated hASC: Endothelial Cell Proliferation*

For the cell proliferation assay, $1\times10^4$ cells per well were seeded in 96-well plate in triplicate for each sample. After 24 h of culturing with DMEM with 2% FBS, the cells were washed twice with PBS. The conditioned media from the encapsulated and free cells under hypoxic/normoxic conditions were added to the cells along with equal amount of fresh DMEM media supplemented with 10% FBS. Wells treated with only DMEM with 10% FBS without any stimulation with conditioned media were taken as the control. The cells were grown at 37°C in 5%

$CO_2$ for 4 days followed by MTS cell proliferation assay (Promega) according to manufacturer's protocol.

*Animal Model*

Immunocompetent female Lewis rats (200–250 g, Charles River, QC) were used. All procedures were in compliance with the NIH and Canadian Council on Animal Care guidelines for the use and care of animals.

*Intramyocardial Microcapsule Transplantation*

The rats were maintained on standard rat chow diet. Myocardial infarction was induced by occlusion of the left anterior descending coronary artery (LAD) as described previously (2,5). Female Lewis rats were anesthetized using 5% isoflurane in an induction chamber. The rats were intubated with an 18-G catheter, ventilated at 80 breaths/min under anesthetic condition. A left thoracotomy was performed through the fourth intercostal space to expose the left ventricle. The left coronary artery was ligated 2 mm from its origin with a 7–0 polypropylene suture (Ethicon, Inc., Somerville, NJ). The ischemic myocardial segment rapidly became identifiable through its pallor and akinesia. Fifteen minutes after ligation of the artery, three 50-µl intramyocardial injections in the peri-infarct area of the left ventricle were given groupwise according to Table 1 using a 27-gauge needle.

*Retention of ASCs After 10 Weeks: Detecting the LacZ-Labeled Cells*

Histological assessments of the left ventricular hearts were performed on rats after 10 weeks of myocardial transplantation of LacZ-labeled hASCs. Hearts were stained for evidence of cell engraftment using β-galactosidase. For β-galactosidase activity, hearts were added to a solution containing 1 mg/ml 5-bromo-4-chloro-3-indoyl-β-D-galactoside (X-gal), 2% dimethylsulfoxide, 20 mM $K_3Fe(CN)_6$, 20 mM $K_3Fe(CN)_6.3H_2O$ and 2 mM magnesium chloride, 0.02% Nonidet P40, and 0.01% deoxycholate (5). The specimens were incubated in a 37°C incubator with a humidified atmosphere of 5% $CO_2$ for 8 h. They were then washed with PBS and fixed in 2% paraformaldehyde overnight. After fixation, the myocardium was embedded in paraffin. Ribbon sections of tissue were cut on microtome and stained with eosin dye to detect cell cytoplasm.

*Retention of ADSCs After 10 Weeks: Polymerase Chain Reaction Analysis*

Random samples were selected from each group for polymerase chain reaction analysis to confirm the survival of the implanted male hASCs in the female rat hearts at week 10. Genomic DNA was purified using DNeasy (Qiagen, Valencia, CA) according to the manufacturer's instructions, and the presence of living human male cells in female rat hearts were confirmed by targeting a specific microsatellite sequence within the human Y chromosome (DYS390). PCR was performed on equal amount of extracted DNA using Taq DNA Polymerase (Invitrogen). To detect specific gene product, the primer pair used was forward primer 5′TATATTTTACACATTTTTGGGCC3′ and reverse primer 5′TGACAGTAAAATGAACACATTGC3′ with an amplicon size of 250 bp (3,19). Amplifications were carried out for 30 cycles at 94°C for 15 s (denaturation), 54°C for 20 s (annealing), and 72°C for 20 s (extension).

*Myocardial Infarct Area Analysis*

Ten weeks after myocardial infarction, rats were deeply anesthetized and sacrificed by rapid excision of the heart. The excised hearts were immediately soaked in cold saline to remove excess blood from the ventricles and fixed in neutral-buffered 4% formalin. Paraffin-embedded samples were sectioned at 5 µm, and Masson's trichrome staining (DBS, Pleasanton, CA) was performed to delineate scar tissue (blue color) from the total area of myocardium (39). Masson's trichrome-stained sections were captured as digital images and analyzed by ImageJ-1.41 software. Infarct area, epicardial and endocardial length of infarction, and ventricular and septal wall thickness were calculated and expressed as a percentage.

*Immunohistochemistry for Detecting Neovascularization*

Neovascularization was evaluated by analyzing the capillary and arteriole density in the peri-infarct area. For this, immunohistochemical staining was performed with antibodies against platelet endothelial cell adhesion molecule (PECAM; Santa Cruz) for identification of

**Table 1.** Animal Experimental Groups and Their Abbreviations

| Groups (No. of Animals ) | Samples | Abbreviations |
|---|---|---|
| Group 1 ($n=4$) | Sham (control) | S |
| Group 2 ($n=8$) | Empty microcapsules (control) | M |
| Group 3 ($n=8$) | Free hASCs ($1.5\times10^6$) | FC |
| Group 4 ($n=8$) | Microcapsulated hASCs ($1.5\times10^6$) | MC |

The cells used for myocardial transplantation were LacZ-labeled male human adipose stem cells (hASCs).

endothelial cells and smooth muscle α-actin (Santa Cruz) for tracing the smooth muscle cells. Briefly, for measurement of capillary density, five fields in the peri-infarct area were imaged with 200× magnification and average numbers of capillaries with less than 10 μm diameter were counted. The capillary density was quantified as the (mean total PECAM-positive microvessels)/mm$^2$ using three tissue sections spanning per-infarct tissue region of each animal. Similarly, arteriole densities were quantified as the (mean total smooth muscle α-actin-positive microvessels)/mm$^2$.

*Echocardiography and Cardiac Performance*

Transthoracic echocardiography was performed on all surviving animals in the four groups before operation (baseline) and before sacrifice on week 10. Echocardiograms were obtained with a commercially available system (SonoSite, Titan-Washington, Seattle, WA) equipped with a 15-MHz transducer, according to the American Society of Echocardiology leading-edge method (5). After sedating the animals, left ventricular end-diastolic (LVEDD) and end-systolic (LVESD) diameters were measured with M-mode tracings between the anterior and posterior walls from the short-axis view just below the level of the papillary muscles of the mitral valve. Two images were obtained in each view and averaged over three consecutive cardiac cycles. Fractional shortening (FS) was determined as [(LVEDD − LVESD) / LVEDD] × 100 (%). All measurements were performed by one experienced observer who was blinded to the treatment groups.

*Statistical Analysis*

All data are expressed as mean ± standard deviation (SD). Multiple group comparison was performed by one-way analysis of variance (ANOVA) followed by post hoc analysis using the Bonferroni procedure for multiple comparison of means. Values of $p < 0.05$ were considered to be statistically significant.

## RESULTS

*Characteristics of the GCAC Microcapsules Encapsulating hASCs*

The reaction between chitosan and genipin occurred moderately after mixing the two solutions and could be monitored by detecting the changes in the physical appearance of the mixture from time to time. Results in Figure 2 exemplifies that the chitosan-genipin reaction generated a fluorescent bright circle circumscribing each microsphere core after 12 h of exposure of the AC capsule to genipin, which was not detected in the one that was not exposed to genipin. This is in accordance to our earlier results (7,8). Figure 2 (bottom) shows the fluorescence profile corresponding to the line across the optical section of the microcapsules. It was clear that the intensity of the inner alginate cores was similar to that of the background signals, whereas peaks corresponding to the fluorescence of the microcapsule membrane appeared with the relatively higher intensity at the capsular surface. The cells were also viable in both AC and GCAC capsules, as detected by calcein staining. Bright field picture of the cell containing microcapsules show that they were generally spherical and uniform in shape and size, with an average diameter of about 200 μm. Figure 3 shows that the mesh-like porous internal morphology of blank microcapsule (Fig. 3A, B). The morphology of the cell-loaded microcapsules was also similar (Fig. 3C) to the empty one, confirming that the internal structure of the microcapsules was not influenced by the hASC loading.

Viability of the hASCs was also assessed at regular intervals using polyanionic calcein AM and ethidium homopolymer EthD-III dyes. Figure 4 is a representative example of the encapsulated cells showing calcein-stained encapsulated viable cells and EthD-III-stained dead cells on day 21. The fluorescent outer circles of GCAC microcapsules, due to genipin-chitosan cross-linking, also disappeared after day 21. This indicates that the outer surface has gradually started disintegrating, although the exact time of degradation was not analyzed in this study.

*Efficient Release of hVEGF Molecules From Encapsulated hASCs Under Hypoxic Conditions*

In order to understand the therapeutic potential of encapsulated cells in infarcted heart, we checked the VEGF release potential of the encapsulated cells under hypoxic condition, which is a very prevalent condition in an ischemic myocardial environment. The data in Figure 5 show that, under hypoxic condition, the encapsulated cells secretes significantly increased amount of VEGF at 24 h (6.02 ng/4 × 10$^6$ cells vs. 3.85 ng/4 × 10$^6$ cells; $p < 0.05$), 48 h (16.21 ng/4 × 10$^6$ cells vs. 4.63 ng/4 × 10$^6$ cells; $p < 0.05$), and 96 h (20.58 ng/4 × 10$^6$ cells vs. 6.1 ng/4 × 10$^6$ cells; $p < 0.05$) in comparison to that under normoxic conditions.

*hVEGF Released From Encapsulated hASCs Have Mitotic Effect on Endothelial Cells*

To check the biological activity of the released protein, a HUVEC proliferation assay was performed on the released conditioned media from 96 h hypoxic and normoxic hASC encapsulated samples. The samples with high VEGF concentrations, that is, from hypoxic conditioned media from free and encapsulated cells, significantly increased the proliferation rate of HUVECs

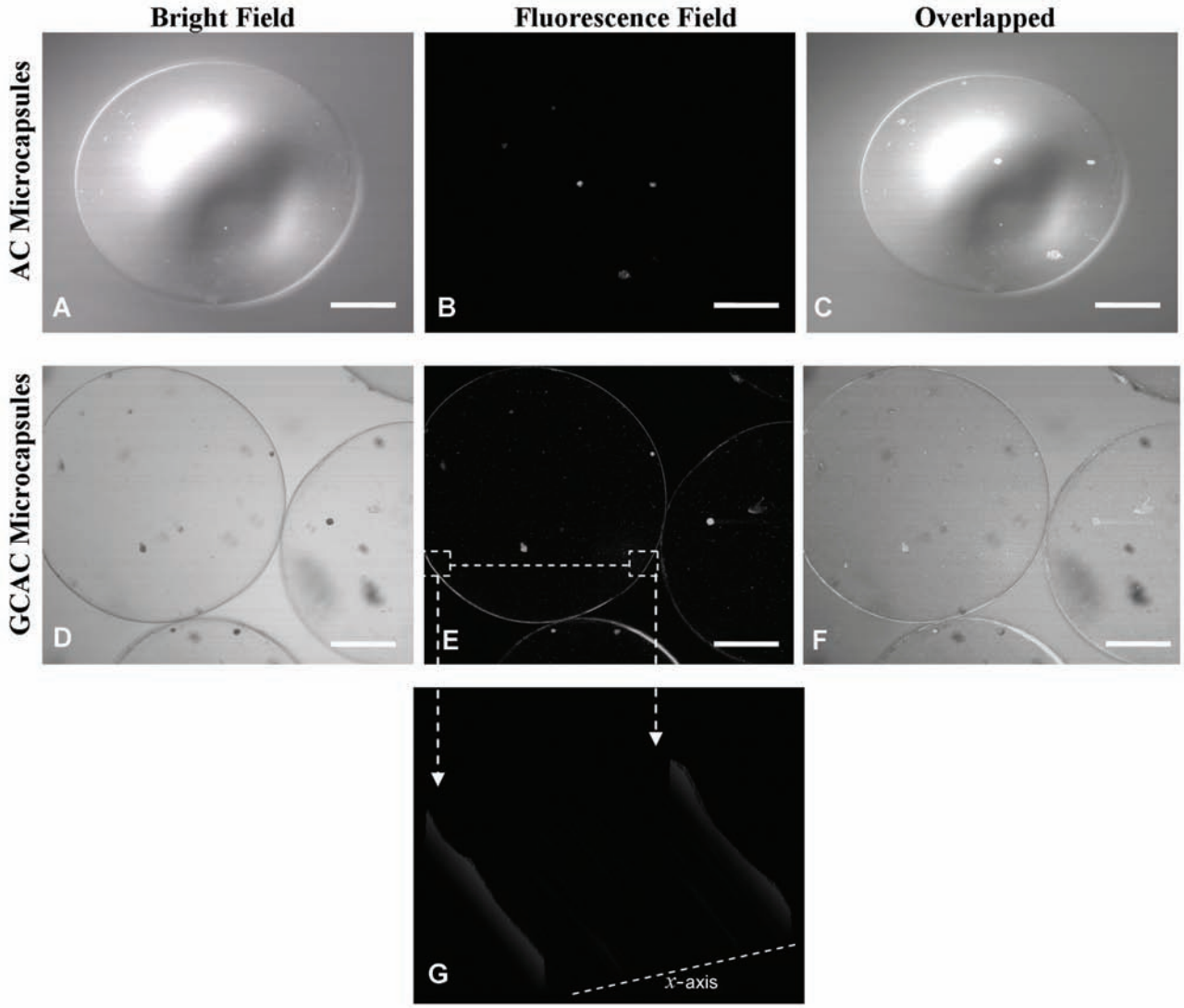


**Figure 2.** Confirmation of reaction between chitosan layer and outer genipin coating in preparing genipin-cross-linked alginate chitosan (GCAC) microcapsules using confocal microscope. The above figure represents the confocal laser scanning microscopic images of the AC (A–C) and GCAC microcapsules (D–F) at an excitation of 488 nm and emission of 530 nm. The microcapsular AC membrane was cross-linked with genipin (5.0 mg/ml) at 37°C for 12 h. The bright fluorescence on the outer surface of the GCAC capsules indicates the complete cross-linking between genipin and chitosan. This fluorescence was not there in AC capsules that were no treated with genipin. The encapsulated viable cells, stained by calcein AM, are shown as the dots inside the capsule. Scale bar: 50 μm. (G) Fluorescence intensity profile corresponding to the white dotted *x*-axis line drawn across the plane of the GCAC microcapsules using ImageJ-1.43 m.

in comparison to that from normoxic conditioned media (163% in hypoxic free and 154.5% in hypoxic encapsulated cells against 31% proliferation in control; 100% proliferation was taken as baseline for normoxic free cells) as illustrated in Figure 6. Under hypoxic condition, conditioned media from both encapsulated and nonencapsulated cells induced around fivefold cell proliferation compared to the unstimulated control, while under normoxic condition the proliferation was around 3.3-fold in both cases. Thus, the extent of cell proliferation was directly proportional to the released VEGF amount by the hASCs under different conditions.

### *Higher Retention and Survival Rate of Transplanted Cells Using GCAC Microcapsules*

To analyze whether the microcapsules were able to protect the cells against the harsh external beating environment in the heart, harvested heart tissue samples were stained with X-gal in order to trace the transplanted LacZ gene containing cells in the heart. The picture in Figure 7A

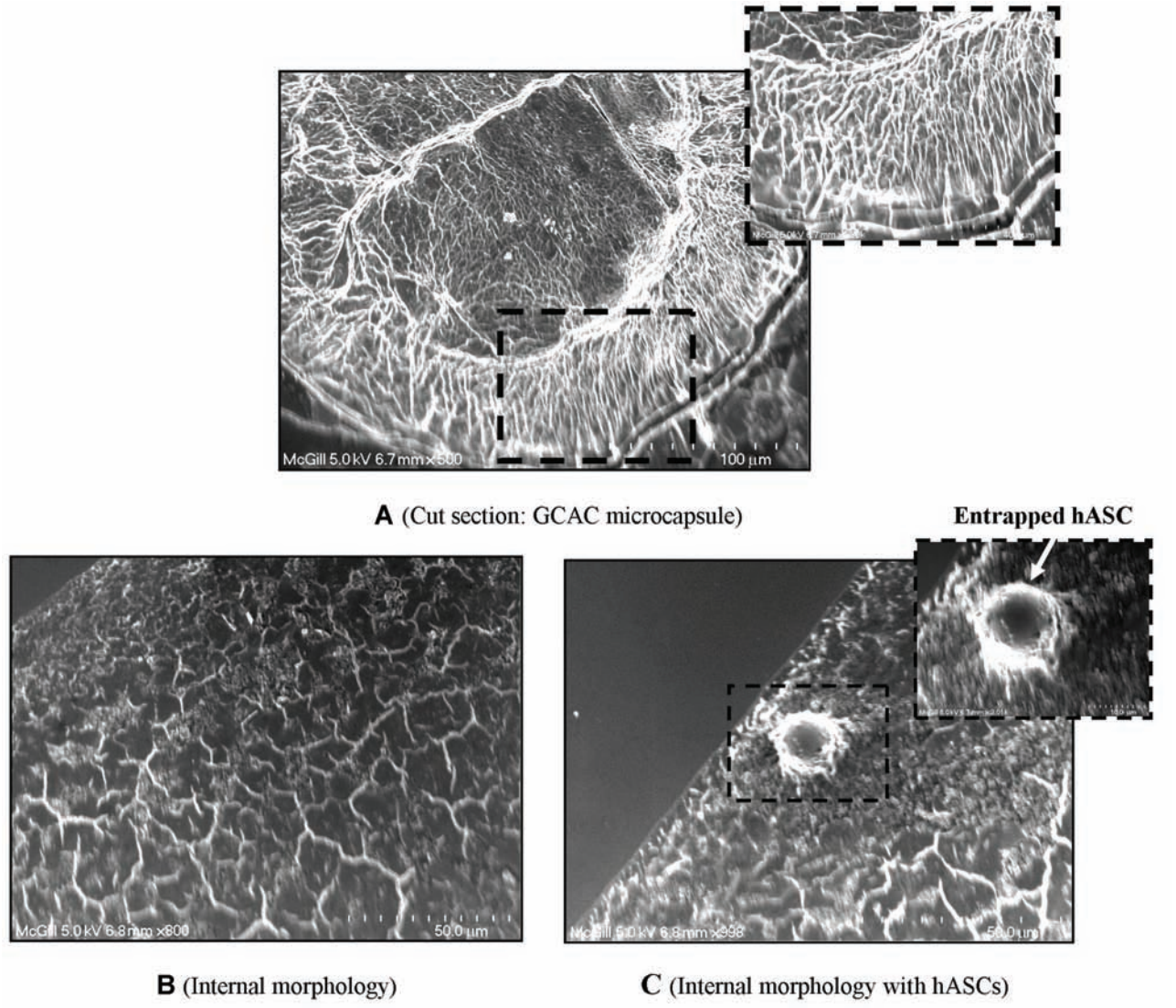


**Figure 3.** Scanning electron microscope images of microcapsules with and without hASCs. Images of internal morphology of cell loaded with genipin-cross-linked alginate chitosan (GCAC) microcapsules (A; scale bar: 100 µm; original magnification: 500×) with subset showing a higher magnification (1,300×) of the capsular outer membrane (scale bar: 40 µm). The microphotograph at the bottom represents the internal mesh-like scaffold structure of the empty GCAC microcapsule (B; scale bar: 50 µm; original magnification: 800×) and hASC loaded GCAC microcapsule (C; scale bar: 50 µm; original magnification: 800×) with the subset showing the magnified image of the entrapped cell within the capsular scaffold (scale bar: 10 µm; original magnification: 3,013×).

gives us a qualitative idea of the amount of encapsulated cells survived in the heart in comparison to free ones. Although the retention of cells were higher in the encapsulated group, there was no trace of the polymeric capsules after 10 weeks, which probably got degraded and bioresorped in the body over time leaving the cells behind. The infarct and peri-infarct portions of the heart tissues were also used for DNA extraction. This was used to detect the presence of Y chromosome of transplanted hASC in the female rat heart using standard PCR. Equal amounts of tissue samples from the peri-infarct region of heart were taken for DNA extraction. The gel electrophoresis of the PCR products shows a clear distinction in band intensities of encapsulated and free cells (Fig. 7B). The encapsulated cells showed 3.54 times more retention of viable transplanted cells in the heart in comparison to nonencapsulated cells (100% vs. 28.2%; $p < 0.05$) as quantified by relative band intensities using ImageJ software. This semiquantitative analysis suggests that, using microencapsulation technology, we need less cell number to achieve desirable cell retention at the target site.

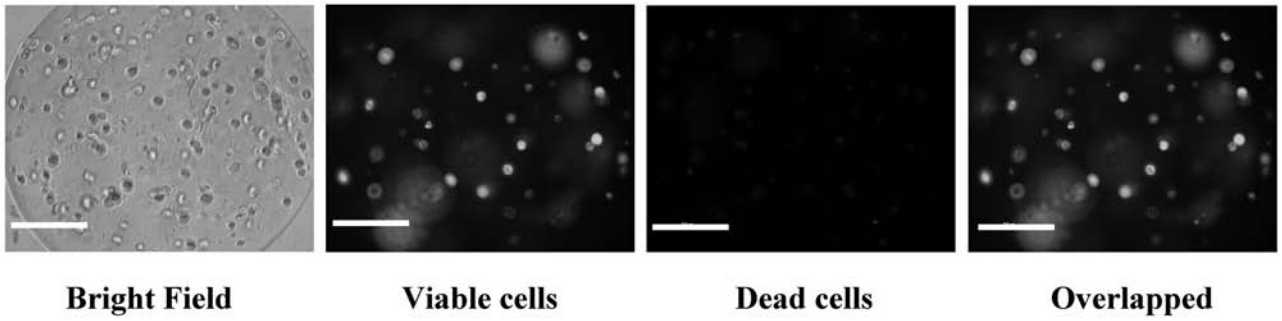


**Figure 4.** Viability of microencapsulated stem cells after 21 days of culture in DMEM supplemented with 10% FBS at 37°C. Viability tests were done by using the calcein AM and ethidium homopolymer dye. Representative bright field and fluorescent images of a capsule encapsulating the cells under 400× magnifications in a fluorescence microscope. Scale bar: 50 μm.

*Microencapsulated hASCs Efficiently Reduce Fibrosis in the Infarcted Tissue*

Macroscopic views of Masson's trichrome-stained hearts are shown in Figure 8. In all the groups, stained fibrous infarct areas were clearly observed as gray areas in the heart sections 10 weeks after myocardial infarction. We measured the infarct size and other parameters in the left ventricles at the section of the middle point between ligation and apex as previously described elsewhere (39). As shown in Table 2, the average percentage infarction size in hearts of MC group (21.6% ± 1.1%) was significantly reduced compared to that in control hearts (33.3% ± 3.2% in M and 27.2% ± 3.1% in FC). Thin left ventricular wall with dilated left ventricular cavities (average thickness: 0.86 mm and 1.41 mm) were observed in the M and FC control groups, while the hearts in the MC group had lesser infarcts and thicker left ventricular wall (average thickness: 1.85 mm) than the control hearts. There were also significant differences between the control groups and the FC group with respect to the percentage endocardial infarction length and the percentage epicardial infarction length.

*Induction of Myocardial Angiogenesis and Arteriogenesis*

In this section, we tried to comprehend whether it was the higher angiogenic effect of the microencapsulated

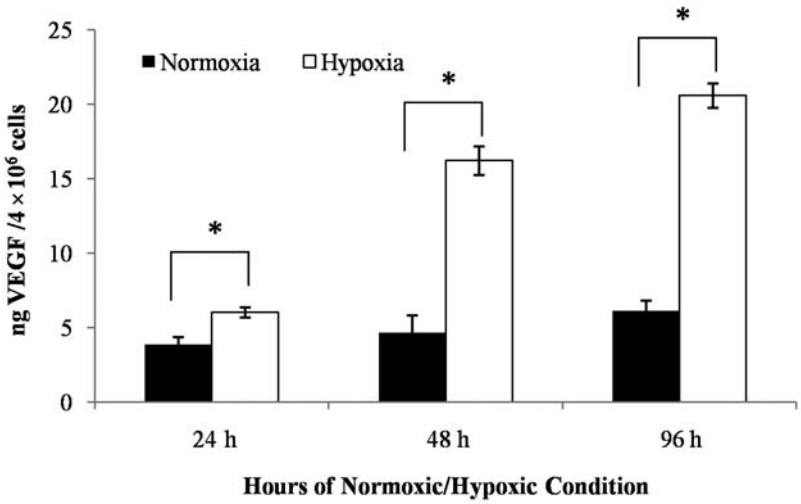


**Figure 5.** Modulation of vascular endothelial growth factor (VEGF) secretion by microencapsulated adipose stem cells under hypoxic and normoxic condition. Secretion of VEGF by GCAC encapsulated hASCs cultured in normoxic or hypoxic conditions over 24, 48, and 96 was measured by ELISA and is presented as mean ± SD nanogram of secreted factor normalized to $4 \times 10^6$ cells at time of harvest. VEGF production in normoxia and hypoxia was compared with one-way ANOVA analysis ($n = 3$; $^*p < 0.05$).

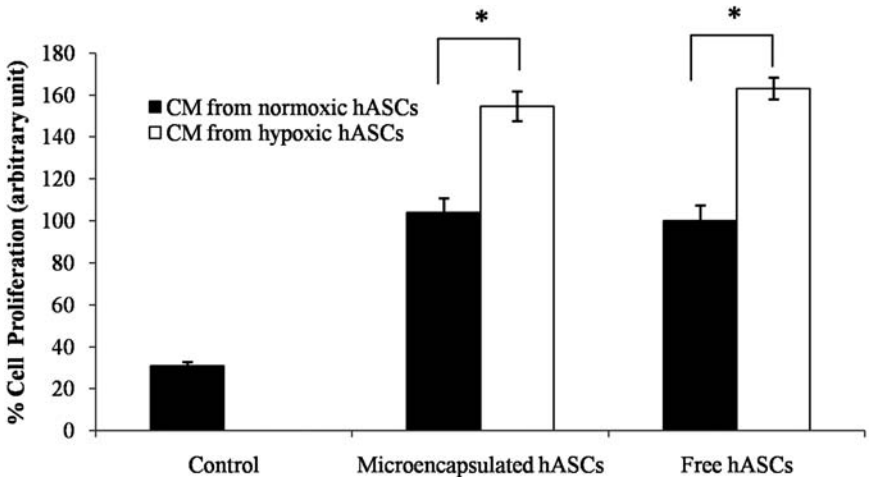


**Figure 6.** Evaluation of bioactivity of released vascular endothelial growth factor (VEGF) from adipose stem cells: endothelial cell proliferation assay. Effects of free and encapsulated hASC supernatants on human umbilical vein endothelial cell (HUVEC) proliferation are represented as percentage of cells on day 4 under hypoxic and normoxic conditions (mean ± SD). For this unstimulated endothelial cells are taken as the control. The average cell number in wells treated with normoxic media from free cells on day 4 of proliferation was taken as 100%, and cells from other wells were normalized to it. Numbers of endothelial cells exposed to normoxic media only are significantly lower than those exposed to hypoxic media. This was same for both free and encapsulated cells. VEGF production in normoxia and hypoxia was compared with one-way ANOVA analysis ($n=3$; $^*p<0.05$).

hASCs that was responsible for the scar area reduction in treatment groups. We assessed the neovasculature formation in the peri-infarct area by detecting the capillary (Fig. 9A–D) and artery densities (Fig. 9E–H). As shown in Figure 9I**,** we noticed a significant improvement in angiogenesis in the FC and MC groups compared to the M ($197 \pm 24.1/mm^2$ for MC, $144.4 \pm 15.45/mm^2$ for FC vs. $67.33 \pm 17.7/mm^2$ for control, $p<0.01$). Moreover, MC group also showed significantly higher capillary density compared to FC. Similar results were obtained with arteriole density in MC group ($20.6 \pm 4.9/mm^2$ for MC, $17.5 \pm 3.92/mm^2$ for FC vs. $6.9 \pm 2.01/mm^2$ for control, $p<0.001$) as presented in Figure 9J. Unlike capillary density, MC group showed no significant enhancement in arteriole density compared to FC.

### *Attenuation of the Progression of Cardiac Dysfunction by Microencapsulated hASCs*

Here we assessed the cardiac function 10 weeks after myocardial infarction in the all the four groups by echocardiography. The cardiac functional parameters evaluated by M-mode echocardiography, 10 weeks after LAD ligation, are shown in Figure 10. In the control group (M), significantly decreased fractional shortening was seen, a typical indication of postinfarction cardiac failure. In the group that underwent microencapsulated cell transplantation (MC), significantly higher FS was observed as compared to groups M (group MC: 24.2% ± 2.1%; group FC: 19.1% ± 0.5%; group M: 12.0% ± 4.0%; $p<0.05$). FS data indicate a significant cardiac function improvement in group MC compared to group FC. Thus, the analysis using echocardiographic FS% data suggests that encapsulated hASCs can be a better alternative to free hASCs to improve cardiac function after acute myocardial damage.

## DISCUSSION

Cardiomyocytes are considered to be terminally differentiated cells, and regeneration is limited in adult life (48). Thus, the irreversible damage of infarction in the heart increases the risks of having severe complications such as myocardial wall rupture, arrhythmia, aneurysms, and eventual heart failure (20). Application of mesenchymal stem cell therapy in such cases have become one of the most ardently researched and debated subjects in the last 10 years (13,16,17,46). The essence of mesenchymal stem cells can be explained through three essential characteristics: firstly their multilineage differential potential, secondly their immunomodulatory effect, and thirdly their ability to self-regenerate for an unlimited amount of time (4). In this study, we have used xenogeneic donor mesenchymal stem cells from adipose origin in immunocompetent rats as an alternative to widely used mesenchymal bone marrow stem cells.

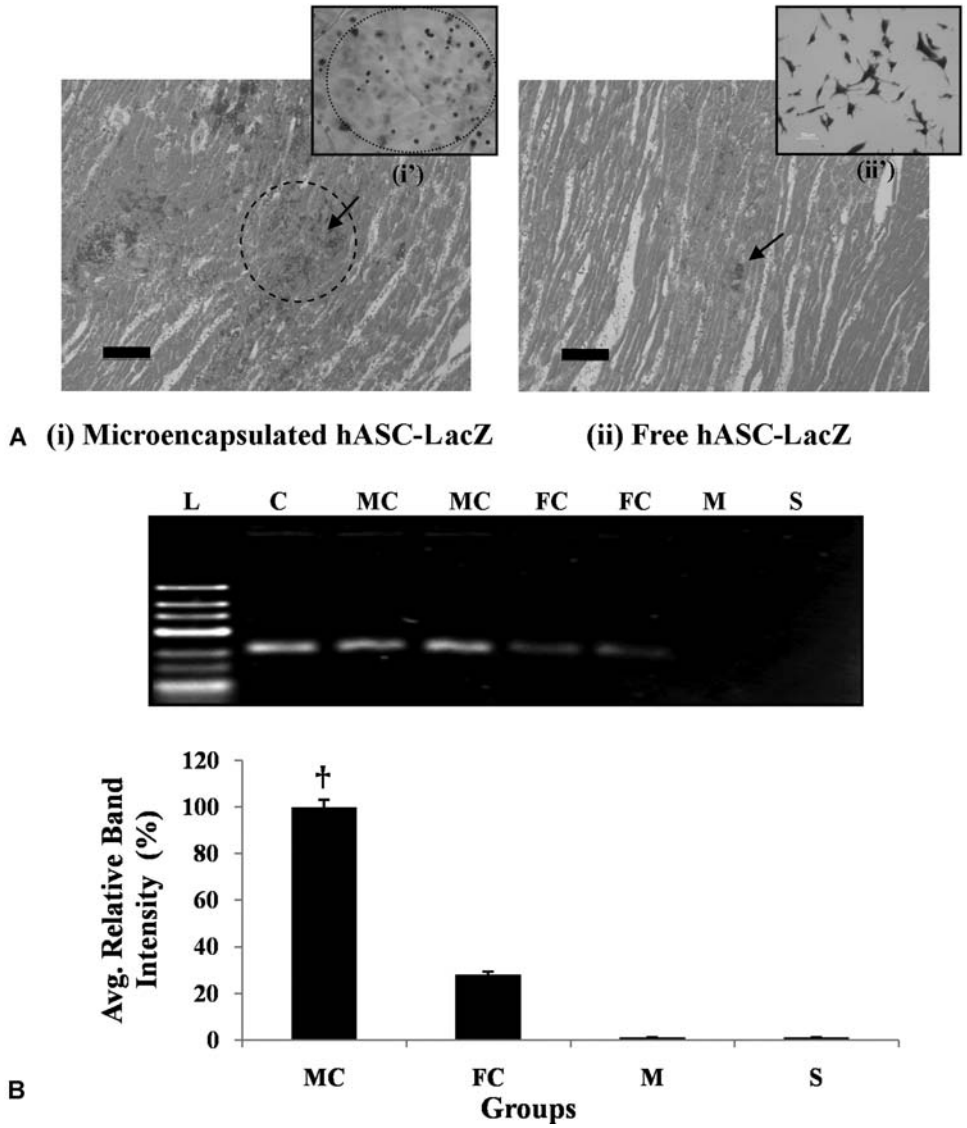


**Figure 7.** Higher retention of adipose stem cells (hASCs) in the left ventricular myocardium using microcapsules 10 weeks post transplantation. Histological sections of the left ventricular heart stained with X-gal in (Ai) encapsulated hASCs group and (Aii) free hASCs group. The transplanted hASCs are indicated by the arrows. (Ai') X-gal stained microencapsulated hASCs, with stable LacZ expression, which were used for transplantation in microencapsulated hASC group. This positive X-gal staining illustrates that the encapsulated cells were viable and express the LacZ transgene from within the microcapsules. (Aii') X-gal stained monolayer hASC culture, stably transduced with LacZ gene, which were used for transplantation in free hASC group. Scale bars: 100 μm. (B) PCR products (250 bp) specific for the human Y chromosome (DYS390 sequence) as detected in 2% agarose gel. There were clear and distinct bands in all the female rat hearts with microencapsulated male hASCs at 10 weeks (MC). These band intensities were much lower in free hASC groups (FC). Two PCR products from each group are shown here. The ImageJ analysis of the band intensities show the FC group with average 28% band intensity taking the band intensity of MC group as 100%. C represents the positive control for the in vitro cultured male hASCs, whereas M represents the negative control for the group M treated with empty microcapsules and S represents the myocardium for the sham group S. †Statistically significant between microencapsulated hASCs and free hASCs.

Apart from direct free cell delivery, micro- and nanoscaffold mediated delivery of stem cells is another widely used approach that has been exploited in the field of regenerative medicine (31). Seeding cells on these scaffolding systems are used to provide a suitable environment for cell colonization, proliferation, and differentiation. Recently, Wei et al. reported the development of a bioengineered cardiac patch composed of a sliced porous biological scaffold inserted with multilayered mesenchymal stem cells for myocardial regeneration (43). An array of biomaterials have been used to create scaffolds including type I collagen, a biocompatible polymer onto which

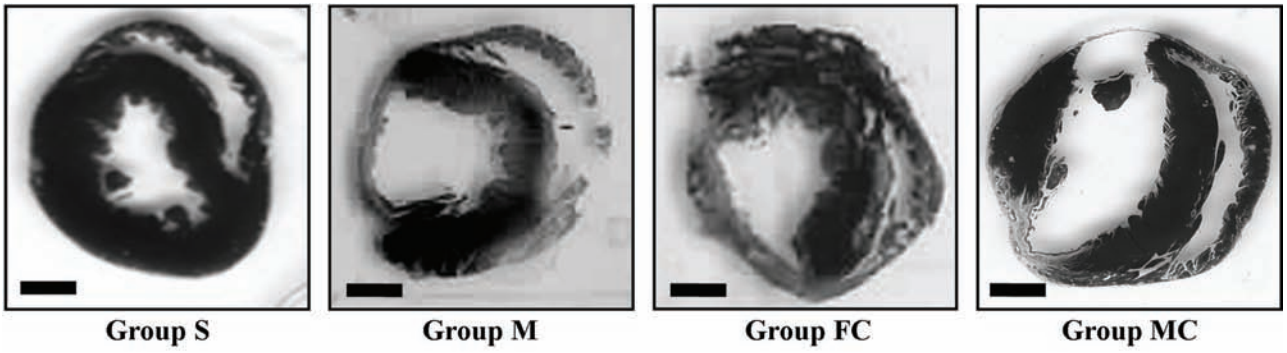


**Figure 8.** Effect of microencapsulated and free human adipose stem cells (hASCs) on infarcted rat heart: scar area detection. Ten weeks after myocardial infarction, the heart was excised and stained using Masson's trichrome staining method where the gray-stained area represents the scar tissues (I: infarcted area in left ventricular wall; II: noninfarcted left ventricular portion; III: septum). Infarct scar area and the total area of LV myocardium measured automatically by the means of ImageJ-1.41 (NIH) software, as shown in subset of Group MC. Gray area represents extracellular matrix (ECM) deposition in scar tissue and bright area represents myocardium. Compared to groups with microcapsules and free hASCs, encapsulated hASC group had less extracellular matrix deposition area. Scale bars: 2 mm.

the cells have a high affinity and poly lactide-*co*-glycolic acid, a biodegradable polymer supporting cell stability (18,22,44,45). In an interesting study, Zhang et al. reported that microencapsulated xenogeneic Chinese hamster ovary cells genetically modified to express VEGF can induce significant therapeutic effects in ischemic heart disease (51). In a similar approach, Goren et al. also reported microencapsulated mesenchymal stem cells are ideal candidates for hypoimmunogenic long-term cell-based therapy (12). Although microcapsules prepared from alginate and poly-L-lysine polymers are being used extensively for such long time study for their ability to support cell viability, several studies have demonstrated that they lack mechanical strength and stability when applied over the long term in vivo, leading to leakage of the encapsulated cells (25,26,34). Furthermore, the addition of PLL to alginate stimulates necrosis of the encapsulated cells (14,15). As most synthetic polyelectrolyte materials exhibit a moderate level of cell cytotoxicity, naturally occurring materials constitute ideal polymers for live cell encapsulation. In recent years, genipin has drawn considerable research interests as an alternative cross-linker due to its natural origin and low cytotoxicity, allowing for mild but effective chemical cross-linking. Our earlier studies have shown successful encapsulation of liver cells within genipin cross-linked microcapsules for therapeutic applications (7). Preliminary studies (data not shown) show that the empty microcapsules can be intact for at least 10 weeks in the culture media. But once they are entrapping the

**Table 2.** Effect of Microencapsulated Male Human Adipose-Derived Stem Cells (hASCs) on Infarcted Heart: Morphometric Analysis of the Left Ventricle (LV) After Infarction

| Group | Average Infarction Area/ Area at Risk (%) | Average Left Ventricular Wall Thickness (mm) | Epicardial Length of Infarction/ Epicardial Circumference (%) | Endocardial Length of Infarction/ Endocardial Circumference (%) | Heart Weight/ Body Weight (g/kg) |
|---|---|---|---|---|---|
| S ($n=4$) | No infarction | 2.9±0.4* | No infarction | No infarction | 3.7±0.08* |
| M ($n=8$) | 33.3±3.2 | 0.86±0.17 | 47.4±1.05 | 61.5±4.32 | 4.3±0.05 |
| FC ($n=8$) | 27.2±3.1* | 1.41±0.1* | 38.2±3.88* | 53.1±2.02* | 4.05±0.2* |
| MC ($n=8$) | 21.6±1.1*† | 1.85±1.3*† | 32.2±2.42*† | 44.7±4.12*† | 3.98±1.1* |

Values indicate the mean±SD ($n=8$; $n=4$ for sham). Rats were sacrificed 10 weeks after myocardial infarction. All parameters were measured on the midline horizontal sections between ligation point and apex of heart and calculated according to the following formulae: % infarct size=infarct area/total LV area×100; % endocardial infarct length=endocardial length of infarction/endocardial circumference of LV×100; % epicardial infarct length=epicardial length of infarction/epicardial circumference of LV×100.

*Statistically significant compared to control (microcapsules only).

†Statistically significant between microencapsulated hASCs and free hASCs.

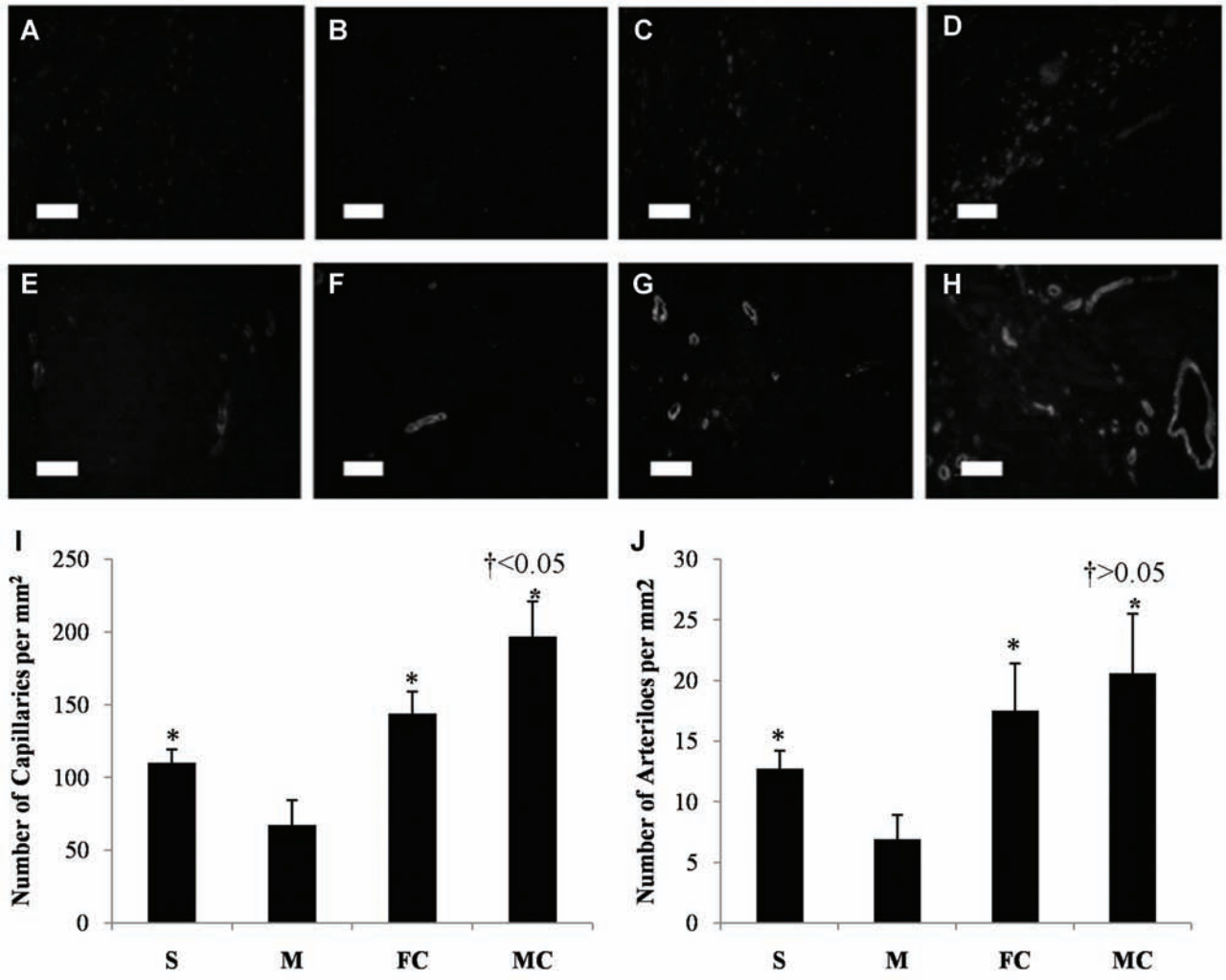


**Figure 9.** Angiogenesis and arteriogenesis in the peri-infarct area. Immunohistological staining of platelet endothelial cell adhesion molecule (PECAM) to detect endothelial cells in (A) Sham, (B) M, (C) FC, and (D) MC groups. Immunohistological staining of smooth muscle α-actin for smooth muscle cells in (E) S, (F) M, (G) FC, and (H) MC groups. Scale bar: 50 μm. Quantification of (I) capillary and (J) arteriole density. Data are expressed as mean density ± SD. One-way ANOVA analysis: *statistically significant compared to control (M), †statistical significance between microencapsulated hASCs and free hASCs.

cells, the microcapsules tend to start degrading after 3–4 weeks (Fig. 4). This is because of the proliferation of encapsulated cells under in vitro culture conditions, which is not the case under harsh in vivo external environment. But the in vivo data (Fig. 7) confirm that the polymeric microcapsule completely disappeared after 10 weeks, leaving the entrapped cells in viable condition. This confirms the bioresorbable and nontoxic nature of the degraded products of the polymeric microcapsule. And this transient nature of the microcapsule is desirable; it disappears from the organ once its job is done. In the present study, our results confirm the higher retention potential of microencapsulated hASCs in vivo as shown in Figure 7 and establish the superior features of biocompatible cell containing GCAC microcapsules in improving heart function in an extreme model of xenogeneic mismatch (Table 1 and Fig. 10). An important point while injecting the microcapsules is the needle size, which should not be too small that it breaks the capsules while injecting, at the same time it should not be too big for intramyocardial injection procedure. As it is very difficult to directly quantify the number of transplanted cells in the heart after 10 weeks, we relied on the relative comparison between the experimental groups. Although the number of transplanted cells used here was optimal to treat the rat heart infarction, this number will vary based on the animal models used in the respective studies. By attenuating the contractile dysfunction and

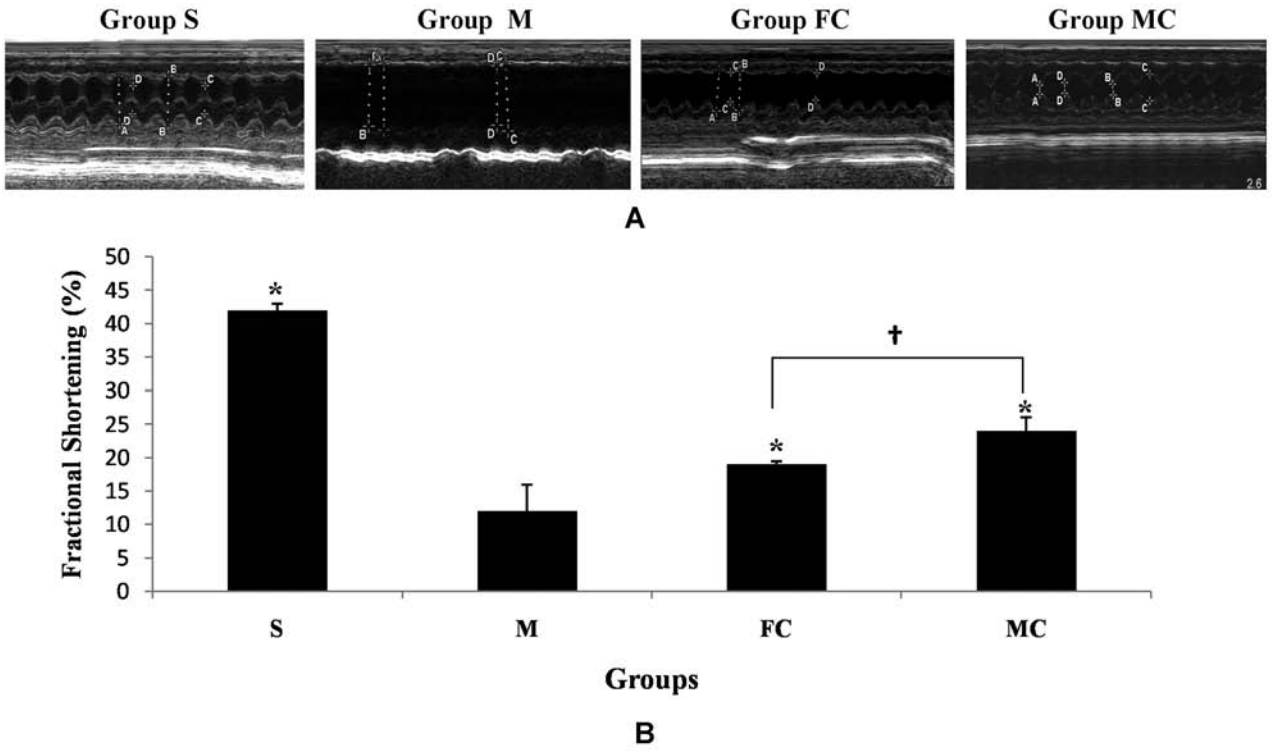


**Figure 10.** Functional effects of microencapsulated and free human adipose stem cells (hASCs) on infarcted rat heart: evaluation of cardiac function by echocardiographic analysis. Ten weeks after myocardial infarction, echocardiography was performed to evaluate cardiac function. (A) M-mode echocardiograms from different groups of rats. Effects of microencapsulated hASCs on left ventricular (LV) fractional shortening on week 10 are also presented (B). Values indicate the mean ± SD ($n = 8$; $n = 4$ for sham). (B) Left ventricular fractional shortening also improved significantly in group MC compared to group M and group FC. *Statistically significant compared to control (microcapsules only). †Statistically significant between microencapsulated hASCs and free hASCs.

pathological remodeling, the microencapsulated hASCs contributed significantly and better than free hASCs to a remarkable recovery in ventricular performance after myocardial infarction.

This is the first study to our knowledge, where hASCs are being successfully encapsulated in polymeric microcapsules and delivered as xenotransplant in immunocompetent rats with acute myocardial infarction. This is also the first time where the GCAC microcapsules have been tested in vivo. The results support our hypothesis that the ASCs, encapsulated in GCAC microcapsules, survive longer and sustain their functional properties in the beating heart compared to free cells, which, in turn, induce reduction of the infarcted scar area and improve cardiac function significantly. Although the encapsulated microcapsules significantly reduced the myocardial infarction in comparison to free cells and untreated groups, the underlying mechanism is not fully understood. It is true that we were able to achieve our goal for better retention of the transplanted viable cells in the infarct area, but we do not know how the encapsulated cells induce its therapeutic effect in vivo. Previous studies have reported the transdifferentiation of ASCs to cardiomyocytes in the cardiovascular environment, while others attribute the improvement in cardiac function to the paracrine activity of stem cells or cell fusion (35,36,42). The in vivo studies of microencapsulated hASCs presented here suggest that vasculogenesis (Fig. 9) can be a probable mechanism of therapeutic action. The in vitro data confirm that microencapsulated cells can effectively induce angiogenesis under hypoxic condition by overexpression of VEGF. VEGF protects the blood vessels from apoptosis, modulates vasomotor response, and supports vessel formation in the ischemic area, thus reducing the infarct size in vivo by improving blood flow (32,52). The results from the present study suggest that the improved heart function is a combinatorial effect of at least two major components—the survival of a significantly higher number of grafted cells even after 10 weeks post transplantation and related angiogenic effects of the implanted cells. In terms of future concern, an elaborate in vivo work is needed to be done to evaluate whether the genipin cross-linked polymeric microcapsules have

any significant effect on the host immune system and on myocardial and serum cytokine profile. Studies are also needed to be done to accurately determine the degradation rate of the GCAC capsules in the in vivo environment. Application of cell-based gene therapy using GCAC microencapsulated genetically modified hASCs to modulate inflammatory effects or promote angiogenesis can be the next step for myocardial treatment (6,38,39,52). Another interesting field of research will be to further enhance the biocompatibility of the GCAC microcapsules by using cyclic arginine-glycine-aspartate (RGD)-conjugated alginate polymers instead of normal alginate, which has shown to help recover cardiac function in infarcted heart (50). To conclude, the present study demonstrates the first successful step to introduce ASCs for improved xenogeneic myocardial transplantation using novel biocompatible and biodegradable microcapsules. Further interdisciplinary research on developing improved cell-entrapped polymeric microcapsules armed with targeting molecules for site-specific delivery will help us bring this technology much closer to clinical applications.

*ACKNOWLEDGMENTS: This work is supported in part by research grant (to D. Shum-Tim and S. Prakash) from Natural Sciences and Engineering Research Council (NSERC), Canada, and Canadian Institutes of Health Research (MOP 64308) to S. Prakash. A. Paul acknowledges the financial support from NSERC Alexander Graham Bell Canada Graduate Scholarship. V.T.S. Rao acknowledges the doctoral fellowship from Fonds Québécois de la Recherche sur la Nature et les Technologies (Quebec, Canada). The authors declare no conflicts of interest.*

## REFERENCES

1. Al Kindi, A.; Ge, Y.; Shum-Tim, D.; Chiu, R. C. J. Cellular cardiomyoplasty: Routes of cell delivery and retention. Front. Biosci. 13:2421–2434; 2008.
2. Al Kindi, A. H.; Chen, G.; Ge, Y.; Bhathena, J.; Chiu, R.; Prakash, S.; Shum-Tim, D. Microencapsulation to reduce mechanical loss of microspheres: Implications in myocardial cell therapy. Can. J. Cardiol. 23:77C; 2007.
3. Atoui, R.; Asenjo, J. F.; Duong, M.; Chen, G.; Chiu, R. C. J.; Shum-Tim, D. Marrow stromal cells as universal donor cells for myocardial regenerative therapy: Their unique immune tolerance. Ann. Thorac. Surg. 85(2):571–580; 2008.
4. Atoui, R.; Shum-Tim, D.; Chiu, R. C. J. Myocardial regenerative therapy: Immunologic basis for the potential "universal donor cells." Ann. Thorac. Surg. 86(1):327–334; 2008.
5. Chen, G. Y.; Nayan, M.; Duong, M.; Asenjo, J. F.; Ge, Y.; Chiu, R. C. J.; Shum-Tim, D. Marrow stromal cells for cell-based therapy: The role of antiinflammatory cytokines in cellular cardiomyoplasty. Ann. Thorac. Surg. 90(1):190–198; 2010.
6. Chen, H. K.; Hung, H. F.; Shyu, K. G.; Wang, B. W.; Sheu, J. R.; Liang, Y. J.; Chang, C. C.; Kuan, P. Combined cord blood stem cells and gene therapy enhances angiogenesis and improves cardiac performance in mouse after acute myocardial infarction. Eur. J. Clin. Invest. 35(11):677–686; 2005.
7. Chen, H. M.; Ouyang, W.; Jones, M.; Metz, T.; Martoni, C.; Haque, T.; Cohen, R.; Lawuyi, B.; Prakash, S. Preparation and characterization of novel polymeric microcapsules for live cell encapsulation and therapy. Cell. Biochem. Biophys. 47(1):159–167; 2007.
8. Chen, H. M.; Ouyang, W.; Lawuyi, B.; Prakash, S. Genipin cross-linked alginate-chitosan microcapsules: Membrane characterization and optimization of cross-linking reaction. Biomacromolecules 7(7):2091–2098; 2006.
9. de Villiers, J. A.; Houreld, N.; Abrahamse, H. Adipose derived stem cells and smooth muscle cells: Implications for regenerative medicine. Stem Cell Rev. Rep. 5(3):256–265; 2009.
10. Gimble, J. M.; Guilak, F. Adipose-derived adult stem cells: Isolation, characterization, and differentiation potential. Cytotherapy 5(5):362–369; 2003.
11. Goldberg, R. J.; Spencer, F. A.; Gore, J. M.; Lessard, D.; Yarzebski, J. Thirty-year trends (1975 to 2005) in the magnitude of, management of, and hospital death rates associated with cardiogenic shock in patients with acute myocardial infarction a population–based perspective. Circulation 119(9):1211–1219; 2009.
12. Goren, A.; Dahan, N.; Goren, E.; Baruch, L.; Machluf, M. Encapsulated human mesenchymal stem cells: A unique hypoimmunogenic platform for long-term cellular therapy. FASEB J. 24(1):22–31; 2010.
13. Hansson, E. M.; Lindsay, M. E.; Chien, K. R. Regeneration next: Toward heart stem cell therapeutics. Cell Stem Cell 5(4):364–377; 2009.
14. Haque, T.; Chen, H.; Ouyang, W.; Martoni, C.; Lawuyi, B.; Urbanska, A. M.; Prakash, S. In vitro study of alginate-chitosan microcapsules: An alternative to liver cell transplants for the treatment of liver failure. Biotechnol. Lett. 27(5):317–322; 2005.
15. Haque, T.; Chen, H.; Ouyang, W.; Martoni, C.; Lawuyi, B.; Urbanska, A. M.; Prakash, S. Superior cell delivery features of poly(ethylene glycol) incorporated alginate, chitosan, and poly-L-lysine microcapsules. Mol. Pharm. 2(1):29–36; 2005.
16. Hare, J. M.; Traverse, J. H.; Henry, T. D.; Dib, N.; Strumpf, R. K.; Schulman, S. P.; Gerstenblith, G.; DeMaria, A. N.; Denktas, A. E.; Gammon, R. S.; Hermiller, J. B.; Reisman, M. A.; Schaer, G. L.; Sherman, W. A randomized, double-blind, placebo-controlled, dose-escalation study of intravenous adult human mesenchymal stem cells (prochymal) after acute myocardial infarction. J. Am. Coll. Cardiol. 54(24):2277–2286; 2009.
17. Hatzistergos, K. E.; Quevedo, H.; Oskouei, B. N.; Hu, Q. H.; Feigenbaum, G. S.; Margitich, I. S.; Mazhari, R.; Boyle, A. J.; Zambrano, J. P.; Rodriguez, J. E.; Dulce, R.; Pattany, P. M.; Valdes, D.; Revilla, C.; Heldman, A. W.; McNiece, I.; Hare, J. M. Bone marrow mesenchymal stem cells stimulate cardiac stem cell proliferation and differentiation. Circ. Res. 107(7):913–920; 2010.
18. Itoi, Y.; Takatori, M.; Hyakusoku, H.; Mizuno, H. Comparison of readily available scaffolds for adipose tissue engineering using adipose-derived stem cells. J. Plast. Reconstr. Aesthet. Surg. 63(5):858–864; 2010.
19. Kayser, M.; Caglia, A.; Corach, D.; Fretwell, N.; Gehrig, C.; Graziosi, G.; Heidorn, F.; Herrmann, S.; Herzog, B.; Hidding, M.; Honda, K.; Jobling, M.; Krawczak, M.; Leim, K.; Meuser, S.; Meyer, E.; Oesterreich, W.; Pandya,

A.; Parson, W.; Penacino, G.; PerezLezaun, A.; Piccinini, A.; Prinz, M.; Schmitt, C.; Schneider, P. M.; Szibor, R.; TeifelGreding, J.; Weichold, G.; deKnijff, P.; Roewer, L. Evaluation of Y-chromosomal STRs: A multicenter study. Int. J. Legal Med. 110(3):125–128; 1997.
20. Knowlton, K. U.; Chien, K. R. Inflammatory pathways and cardiac repair: The affliction of infarction. Nat. Med. 5(10):1122–1123; 1999.
21. Madonna, R.; Geng, Y. J.; De Caterina, R. Adipose tissue-derived stem cells characterization and potential for cardiovascular repair. Arterioscler. Thromb. Vasc. Biol. 29(11):1723–1729; 2009.
22. Mehlhorn, A. T.; Zwingmann, J.; Finkenzeller, G.; Niemeyer, P.; Dauner, M.; Stark, B.; Sudkamp, N. P.; Schmal, H. Chondrogenesis of adipose-derived adult stem cells in a poly-lactide-co-glycolide scaffold. Tissue Eng. Part A 15(5):1159–1167; 2009.
23. Muller-Ehmsen, J.; Whittaker, P.; Kloner, R. A.; Dow, J. S.; Sakoda, T.; Long, T. I.; Laird, P. W.; Kedes, L. Survival and development of neonatal rat cardiomyocytes transplanted into adult myocardium. J. Mol. Cell. Cardiol. 34(2):107–116; 2002.
24. Nguyen, H.; Qian, J. J.; Bhatnagar, R. S.; Li, S. Enhanced cell attachment and osteoblastic activity by P-15 peptide-coated matrix in hydrogels. Biochem. Biophys. Res. Commun. 311(1):179–186; 2003.
25. Orive, G.; Hernandez, R. M.; Rodriguez, G. A.; Calafiore, R.; Chang, T. M.; de, V. P.; Hortelano, G.; Hunkeler, D.; Lacik, I.; Pedraz, J. L. History, challenges and perspectives of cell microencapsulation. Trends Biotechnol. 22(2):87–92; 2004.
26. Orive, G.; Tam, S. K.; Pedraz, J. L.; Halle, J. P. Biocompatibility of alginate-poly-L-lysine microcapsules for cell therapy. Biomaterials 27(20):3691–3700; 2006.
27. Parker, A. M.; Katz, A. J. Adipose-derived stem cells for the regeneration of damaged tissues. Expert Opin. Biol. Ther. 6(6):567–578; 2006.
28. Paul, A.; Ge, Y.; Prakash, S.; Shum-Tim, D. Microencapsulated stem cells for tissue repairing: Implications in cell-based myocardial therapy. Regen. Med. 4(5):733–745; 2009.
29. Paul, A.; Shum-Tim, D.; Prakash, S. Investigation on PEG integrated alginate-chitosan microcapsules for myocardial therapy using marrow stem cells genetically modified by recombinant baculovirus. Cardiovasc. Eng. Technol. 1(2):154–164; 2010.
30. Prakash, S.; Chang, T. M. S. Microencapsulated genetically engineered live E-coli DH5 cells administered orally to maintain normal plasma urea level in uremic rats. Nat. Med. 2(8):883–887; 1996.
31. Prakash, S.; Khan, A.; Paul, A. Nanoscaffold based stem cell regeneration therapy: Recent advancement and future potential. Expert Opin. Biol. Ther. 10(12):1649–1661; 2010.
32. Rehman, J.; Traktuev, D.; Li, J. L.; Merfeld-Clauss, S.; Temm-Grove, C. J.; Bovenkerk, J. E.; Pell, C. L.; Johnstone, B. H.; Considine, R. V.; March, K. L. Secretion of angiogenic and antiapoptotic factors by human adipose stromal cells. Circulation 109(10):1292–1298; 2004.
33. Retuerto, M. A.; Schalch, P.; Patejunas, G.; Carbray, J.; Liu, N. X.; Esser, K.; Crystal, R. G.; Rosengart, T. K. Angiogenic pretreatment improves the efficacy of cellular cardiomyoplasty performed with fetal cardiomyocyte implantation. J. Thorac. Cardiovasc. Surg. 127(4):1041–1050; 2004.
34. Rokstad, A. M.; Holtan, S.; Strand, B.; Steinkjer, B.; Ryan, L.; Kulseng, B.; Skjak-Braek, G.; Espevik, T. Microencapsulation of cells producing therapeutic proteins: Optimizing cell growth and secretion. Cell Transplant. 11(4):313–324; 2002.
35. Sanz-Ruiz, R.; Fernandez-Santos, E.; Dominguez-Munoa, M.; Parma, R.; Villa, A.; Fernandez, L.; Sanchez, P. L.; Fernandez-Aviles, F. Early translation of adipose-derived cell therapy for cardiovascular disease. Cell Transplant. 18(3):245–254; 2009.
36. Song, S. Y.; Chung, H. M.; Sung, J. H. The pivotal role of VEGF in adipose-derived-stem-cell-mediated regeneration. Expert Opin. Biol. Ther. 10(11):1529–1537; 2010.
37. Sterodimas, A.; de Faria, J.; Nicaretta, B.; Pitanguy, I. Tissue engineering with adipose-derived stem cells (ADSCs): Current and future applications. J. Plast. Reconstr. Aesthet. Surg. 63(11):1886–1892; 2010.
38. Stumpf, C.; Seybold, K.; Petzi, S.; Wasmeier, G.; Raaz, D.; Yilmaz, A.; Anger, T.; Daniel, W. G.; Garlichs, C. D. Interleukin-10 improves left ventricular function in rats with heart failure subsequent to myocardial infarction. Eur. J. Heart Fail. 10(8):733–739; 2008.
39. Takahashi, K.; Ito, Y.; Morikawa, M.; Kobune, M.; Huang, J. H.; Tsukamoto, M.; Sasaki, K.; Nakamura, K.; Dehari, H.; Ikeda, K.; Uchida, H.; Hirai, S.; Abe, T.; Hamada, H. Adenoviral-delivered angiopoietin-1 reduces the infarction and attenuates the progression of cardiac dysfunction in the rat model of acute myocardial infarction. Mol. Ther. 8(4):584–592; 2003.
40. Teng, C. J.; Luo, J.; Chiu, R. C. J.; Shum-Tim, D. Massive mechanical loss of microspheres with direct intramyocardial injection in the beating heart: Implications for cellular cardiomyoplasty. J. Thorac. Cardiovasc. Surg. 132(3):628–632; 2006.
41. van der Bogt, K. E. A.; Schrepfer, S.; Yu, J.; Sheikh, A. Y.; Hoyt, G.; Govaert, J. A.; Velotta, J. B.; Contag, C. H.; Robbins, R. C.; Wu, J. C. Comparison of transplantation of adipose tissue- and bone marrow-derived mesenchymal stem cells in the infarcted heart. Transplantation 87(5):642–652; 2009.
42. Vieira, N. M.; Brandalise, V.; Zucconi, E.; Secco, M.; Strauss, B. E.; Zatz, M. Isolation, characterization, and differentiation potential of canine adipose-derived stem cells. Cell Transplant. 19(3):279–289; 2010.
43. Wei, H. J.; Chen, C. H.; Lee, W. Y.; Chiu, I.; Hwang, S. M.; Lin, W. W.; Huang, C. C.; Yeh, Y. C.; Chang, Y.; Sung, H. W. Bioengineered cardiac patch constructed from multilayered mesenchymal stem cells for myocardial repair. Biomaterials 29(26):3547–3556; 2008.
44. Wei, Y.; Hu, Y.; Hao, W.; Han, Y.; Meng, G.; Zhang, D.; Wu, Z.; Wang, H. A novel injectable scaffold for cartilage tissue engineering using adipose-derived adult stem cells. J. Orthop. Res. 26(1):27–33; 2008.
45. Wei, Y. Y.; Hu, H. Y.; Wang, H. Q.; Wu, Y. S.; Deng, L. F.; Qi, J. Cartilage regeneration of adipose-derived stem cells in a hybrid scaffold from fibrin-modified PLGA. Cell Transplant. 18(2):159–170; 2009.
46. Westrich, J.; Yaeger, P.; He, C.; Stewart, J.; Chen, R.; Seleznik, G.; Larson, S.; Wentworth, B.; O'Callaghan, M.; Wadsworth, S.; Akita, G.; Molnar, G. Factors affecting residence time of mesenchymal stromal cells (msc) injected into the myocardium. Cell Transplant. 19(8):937–948; 2010.
47. Wolff, K. D.; Swaid, S.; Nolte, D.; Bockmann, R. A.; Holzle, F.; Muller-Mai, C. Degradable injectable bone cement in maxillofacial surgery: Indications and clinical experience

in 27 patients. J. Craniomaxillofac. Surg. 32(2):71–79; 2004.
48. Yamada, Y.; Wang, X. D.; Yokoyama, S. I.; Fukuda, N.; Takakura, N. Cardiac progenitor cells in brown adipose tissue repaired damaged myocardium. Biochem. Biophys. Res. Commun. 342(2):662–670; 2006.
49. Yang, F.; Xie, Y. T.; Li, H. W.; Tang, T. T.; Zhang, X. L.; Gan, Y. K.; Zheng, X. B.; Dai, K. R. Human bone marrow-derived stromal cells cultured with a plasma sprayed $CaO–ZrO_2–SiO_2$ coating. J. Biomed. Mater. Res. B Appl. Biomater. 95B(1):192–201; 2010.
50. Yu, J. S.; Du, K. T.; Fang, Q. Z.; Gu, Y. P.; Mihardja, S. S.; Sievers, R. E.; Wu, J. C.; Lee, R. J. The use of human mesenchymal stem cells encapsulated in RGD modified alginate microspheres in the repair of myocardial infarction in the rat. Biomaterials 31(27):7012–7020; 2010.
51. Zhang, H.; Zhu, S. J.; Wang, W.; Wei, Y. J.; Hu, S. S. Transplantation of microencapsulated genetically modified xenogeneic cells augments angiogenesis and improves heart function. Gene Ther. 15(1):40–48; 2008.
52. Zhou, L.; Ma, W.; Yang, Z.; Zhang, F.; Lu, L.; Ding, Z.; Ding, B.; Ha, T.; Gao, X.; Li, C. VEGF165 and angiopoietin-1 decreased myocardium infarct size through phosphatidylinositol-3 kinase and Bcl-2 pathways (vol. 12, p. 196, 2005). Gene Ther. 12(6):552; 2005.